Thai Thu Hien Nguyen[1,*]
Thomas D. Turner[1]
Andrea M. E. Matinong[1]
Ivan Marziano[2]
Robert B. Hammond[1]
Kevin J. Roberts[1]

Measured Growth Rates of Ibuprofen: Comparing Single Crystal and Bulk Suspensions Data

The design of industrial crystallization processes usually employs laboratory-scale experimental data which must be correlated with the full-scale process for effective technology transfer. In this context, the measured growth rates of single crystals of ibuprofen in stagnant ethanolic solutions are compared with data recorded for a population of crystals crystallized in an agitated 7-mL reactor. The single crystal growth rates are found to be rather close to those determined in the agitated reactor, with both being also in good agreement with previously published data at the 750-mL scale, suggesting that studies on single crystals can have utility for the purpose of crystallization process design and optimization.

Supporting Information available online

Keywords: Agitated batch crystallization, Bulk suspensions, Crystal growth rates, Number-weighted mean diameters, Single crystal growth

Received: January 21, 2021; *revised:* March 03, 2021; *accepted:* April 23, 2021

DOI: 10.1002/ceat.202100025

1 Introduction

Understanding and characterizing the growth rate of crystals is a key step in the design of crystallization processes and their implementation into commercial manufacturing. Growth rate anisotropy between the individual crystal faces (*hkl*) can strongly influence the resultant morphology and surface chemistry of the particles produced [1] and hence through this affect the physical properties of, e.g., solid, active pharmaceutical ingredients (APIs), which in turn can influence important product attributes such as their bioavailability, wettability, and flowability. Variation in crystal size and shape associated with crystal growth rate dispersion [2–4] can also play an important role in terms of introducing variability into the performance of crystals in many practical formulations. Hence, the measurement of reliable crystal growth kinetic data in the early stages of the drug product development process can be important in terms of estimating the crystal shape, and size distributions, and their dependence on process conditions during scale-up from laboratory to manufacturing operations.

Growth rate data at the laboratory scale can be measured both through single crystal growth rate experiments [1, 2, 5–7] and through the assessment of crystal size distributions in agitated suspension crystallization in batch vessels [2, 8–10]. Such correlation between measurements can provide a helpful basis for the assessment of the scale-up of crystallization processes by industry through the use of process modeling methodology [11]. Single-crystal measurement methods, carried out under well-defined conditions, provide an excellent baseline assessment for studying the basic growth kinetics and associated crystal growth mechanism of a solution solute growth system. In particular, these approaches avoid the impact of process-dependent phenomena such as growth rate dispersion and secondary nucleation [12] and attrition associated, e.g., with the collision of crystals with reactor internals or other crystals, all of which may impact upon the crystallization process and its growth kinetics.

However, industrial crystallization is usually carried out in agitated batch reactors. In agitated crystallizers, direct measurement of crystal growth rates can be challenging as the crystals concerned are in continuous motion within the vessel and hence can only be briefly viewed in their projected form [13, 14]. Such measurements can also be adversely impacted by the influence of the spatially varied hydrodynamic environments that are typically involved in industrial crystallizers [15–18], e.g., heat and mass transfer which can vary significantly within the crystallizer environment and can be affected by agitation and mixing effects [19–21]. In particular, high agitation intensity can promote nucleation in supersaturated solutions which can reduce crystal size, whilst no or low intensity agitation [22] may lead to poor mixing resulting in the crystals settling within the reactor and not being able to freely contact and develop within the bulk solution. Such variability

[1]Dr. Thai Thu Hien Nguyen, Dr. Thomas D. Turner, Andrea M. E. Matinong, Dr. Robert B. Hammond, Prof. Kevin J. Roberts
H.Nguyen1@leeds.ac.uk
Centre for the Digital Design of Drug Products, School of Chemical and Process Engineering, University of Leeds, Woodhouse Lane, Leeds, LS2 9JT, UK.

[2]Dr. Ivan Marziano
Pfizer Worldwide Research and Development, Sandwich, CT13 9NJ, UK.

can influence the crystal growth kinetics and hence, the resultant crystal form through variation in the crystal habit, polymorphic form [8], and particle size distribution of the final crystalline product.

A wide range of process analytical techniques have been developed for measuring the growth rates of crystals including microscopy techniques [6, 23–28], hot-stage microscopy [2, 29], on-line high-speed imaging [30], in-situ particle viewer [13, 31, 32], and focused beam reflectance measurement (FBRM) integrated with Fourier transform infrared/attenuated total reflectance spectroscopy (FTIR/ATR) [33, 34]. Despite this, there have been surprisingly few studies so far that have attempted to couple measurements of single-crystal growth behavior with related measurements of crystals grown in agitated crystallizers [35, 36] for the same crystallization system. Moreover, the extent to which the performance of a crystallizer can be predicted from single-crystal measurements alone is unclear.

Reflecting this context, this paper seeks to provide such a cross-correlation between these two different process environments through parallel measurements of both the single crystal growth of RS-ibuprofen in seeded ethanolic solutions and the same when measured at the 7-mL scale within a bulk agitated crystallizer as a function of supersaturation.

2 Materials and Methods

2.1 Materials

RS-Ibuprofen (2-(4-isobutyl-phenyl) propionic acid, $C_{13}H_{18}O_2$, M[1)] = 206.28 g mol^{-1}, melting point 77–78 °C) is a nonsteroidal anti-inflammatory drug (NSAID). RS-Ibuprofen (melting point 75–77 °C, purity ≥ 98 %) was obtained from Tokyo Chemical Industry UK Ltd. The solvent used was 95 % ethanol/water (azeotropic composition of a binary mixture of ethanol and water) from Sigma Aldrich.

2.2 Experimental Apparatus

For single crystal growth measurements, the setup employed [1] comprised an inverted optical polarizing microscope (Olympus Optical IMT-2 or Leica/Leitz DM IL 090-131-002) integrated with a CCD Lumenera Infinity 3.3 megapixel camera, a PC with image analysis software to capture crystal images during the growth process, a jacketed crystallization vessel (34 mm inner diameter, 17 mm height), with a flat optical glass disc at the top and the bottom connected to a Huber ministat chiller.

For bulk suspension crystallization, the growth rate measurements in agitated reactors were carried out in the Technobis Crystalline platform [37] which is a laboratory platform including eight temperature-controlled 7-mL scale reactors, each fitted with a three-blade impeller. Each reactor is equipped with a camera (2× magnification lens) which enables visual monitoring of the crystallization process together with a turbidimetric sensor for detecting dissolution and crystallization onset.

2.3 Experimental Methods

Experiments were designed based on previously reported solubility data of RS-ibuprofen in the mixture of 95 % ethanol and 5 % water [1]. An amount of 7 mL of ibuprofen in ethanol at a concentration of 0.98 g mL^{-1} was prepared and kept at a constant temperature of 27 °C and 28 °C (supersaturation level of 0.157 and 0.105, respectively). Measurements were repeated to check the reproducibility of the data.

The single-crystal growth rates of ibuprofen were measured from seeded batch crystallization experiments within supersaturated solutions. The solutions were maintained at a constant temperature of 27 °C and 28 °C, respectively, for 30 min to ensure the temperature of the solution had reached thermal equilibrium. Seed crystals were introduced to a stagnant solution and a sequence of crystal images was captured to measure the overall crystal growth rate, using two to three crystals for each experiment at a defined supersaturation.

Growth rate measurements in the agitated vessel were derived also from seeded batch crystallization experiments within supersaturated solutions. The solutions were heated to 10 °C above the saturation temperature for 1 h to ensure full dissolution of the solute and then cooled to 27 °C and 28 °C, respectively, at a cooling rate of 10 °C per minute and the system was left at constant temperature for 20 min before adding 0.1 wt % of crystal seeds of the weight of ibuprofen in the solution. Images were captured frequently every 10 s. This allowed images which captured clear and sharp crystal edges to be selected for the growth rate estimation in order to obtain crystal size distribution data and hence the overall crystal growth rates.

2.4 Data Analysis

Since the thickness of the ibuprofen crystal in the x-direction is far smaller than the other two (y and z) directions, the crystals in the experiment were only visible normal to the x-axis.

For the single crystal growth experiments, the growth rate of individual crystals was directly calculated from the dimensions of the observed crystals notably a_1, a_2, b_1, b_2, h_1, and h_2 were measured (Fig. 1).

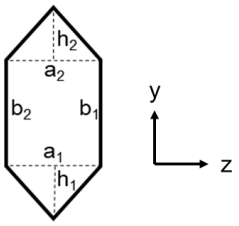

Figure 1. Schematic highlighting the method used for the calculation of the projected area for single crystals, indicating the critical dimensions measured during the data analysis steps for the purpose of calculating the crystallite growth rate.

1) List of symbols at the end of the paper.

The area and the area equivalent diameter of a crystal can be calculated as:

$$A = \frac{1}{2}a_1h_1 + \frac{1}{2}a_2h_2 + \left[\frac{1}{2}(a_1 + a_2)\right]\left[\frac{1}{2}(b_1 + b_2)\right] \quad (1)$$

From the calculated area of the crystals as a function of time, the diameter D for the sphere with the same area as the particle (the area equivalent diameter) versus time was calculated to obtain the growth rate as a function of supersaturation.

$$D = 2\sqrt{\frac{A}{\pi}} \quad (2)$$

For bulk suspension crystal growth rate measurements, image analysis software [37] was used to calculate the projected surface area of the crystals and from this the equivalent diameter of a projected sphere having the same number of pixels and from which the number-weighted mean diameter was determined.

In this, the number mean $\overline{D}$ was calculated by:

$$\bar{D} = \frac{\sum_1^n D_i x_i}{\sum_1^n x_i} \quad (3)$$

where D_i is the particle size given as equivalent diameter and x_i is the number of particles in each particle size range.

The crystal size based on the number weighted mean diameter was plotted as a function of time and supersaturation. The slopes obtained from the linear equations were used to determine the growth rates for each run and plotted as a function of solution supersaturation.

3 Results and Discussion

An example of a sequence of images of crystals grown from ethanol in a 7-mL non-agitated jacketed vessel at σ = 0.157 is displayed in Fig. 2 and the plots of the calculated spherical equivalent diameter versus time are illustrated in Fig. 3, with the data being summarized in Tab. 1 (column 2). Each line represents the growth rate of individual crystals over time.

The slopes of the linear plots reveal the values of the growth rate and show that the particle sizes are similar for both experiments starting at around 100–150 µm at the start of each data collection. The crystal growth rates were found to display a good linear fit with time for each crystal indicating that each crystal appears to develop at constant growth rate for a given supersaturation. However, some variation in the growth rates between different single crystals growing under the same conditions in a non-agitated vessel was observed in this study (Figs. 2 and 3).

A sequence of images of crystals grown from ethanol solutions in the agitated crystallizers is indicated in Fig. 4 and the mean number particle size is given in Fig. 5 with the data summarized in Tab. 1 (column 3).

The ibuprofen crystals obtained during these experiments were of a plate-like hexagonal morphology, as illustrated in Fig. 4, and were found to be consistent in shape with published data [1, 23, 38–40]. The growth rate of the (001) and (011) faces are responsible for defining the in-plane shape of the crystals [1]. In addition, the online images demonstrate that after 5–6 min from seeding the solutions in agitated reactors

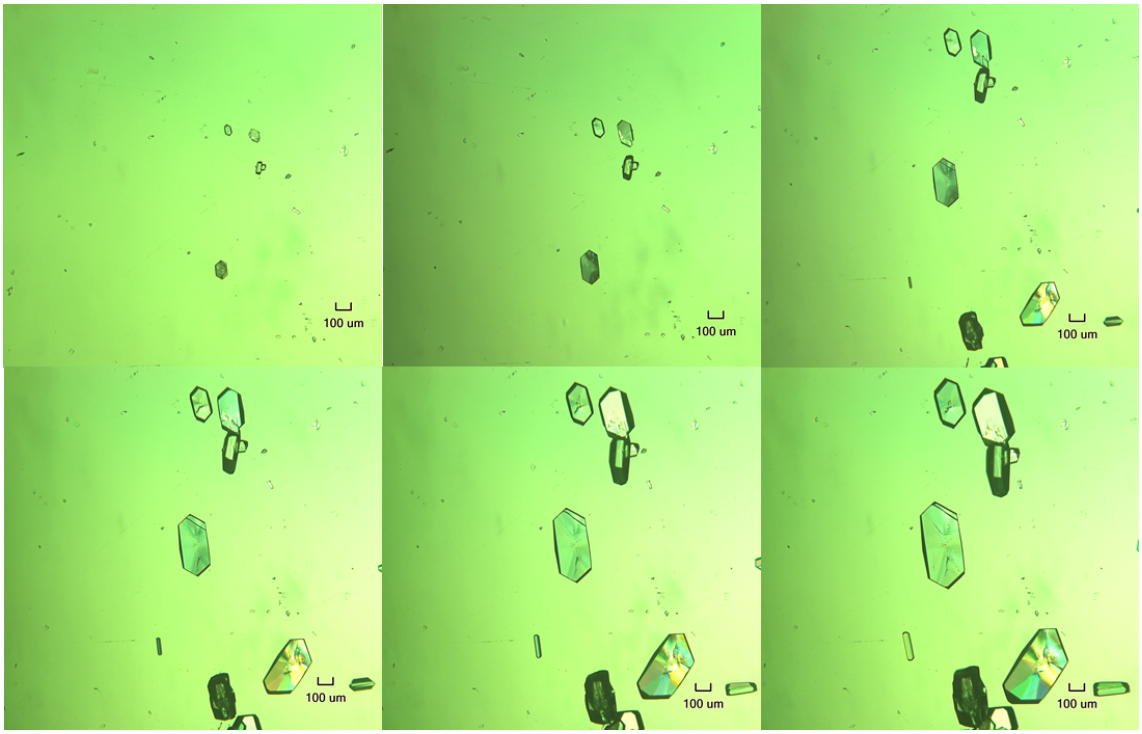

Figure 2. Series of optical micrographs of single crystal growth behavior in a stagnant 95 % ethanol and 5 % water solution at 7 mL after seeding at σ = 0.157 captured every 20 min. From these data, the projected surface area of the crystals and then the spherical equivalent diameter were calculated. Scale bar: 100 µm.

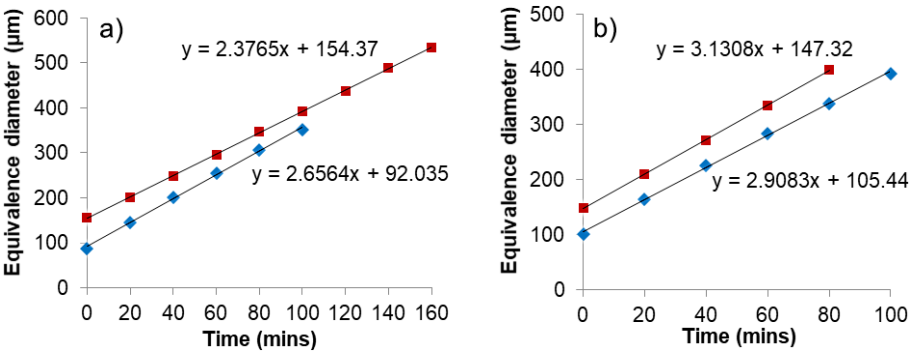

Figure 3. Calculated growth rate (in spherical equivalent diameter) versus time data from experiments in a 7-mL non-agitated jacketed reactor at (a) $\sigma = 0.105$ and (b) $\sigma = 0.157$. The red and blue lines are representative for two repeat runs at each supersaturation.

Table 1. Overall calculated growth rates obtained from single crystal growth experiments in stagnant solutions using microscopy and the calculated growth rate based on the number mean diameter size in the agitated crystallizer at various supersaturation levels, σ.

σ [–]	Overall growth rates [µm min^{-1}]		
	Non-agitated single crystals data 7-mL scale	Agitated vessel data based on mean number diameter 7-mL scale	Data after Rashid [9] 750-mL scale
0.105	2.52 ± 0.20	1.20 ± 0.10	1.57
0.157	3.02 ± 0.71	2.43 ± 0.45	2.35

the captured images rarely showed any crystals. However, following a period of time, there were more new nuclei produced which formed a population of crystals in the crystallizers during the crystallization process.

The data for the growth rate based on the number weighted mean diameter for each supersaturation are given in Fig. 5 and the average growth rates based on the number mean diameter are summarized in Tab. 1.

The summary data of the calculated growth rates for single crystal and agitated batch crystallized measurements are given in Tab. 1 and show that the overall growth rate increases as a function of supersaturation at $\sigma = 0.105$ and 0.157 as expected. This increase in the calculated growth rate trends as a function of supersaturation and gives some confidence that the data treatments are reliable. It was observed that the growth rate measured for the agitated vessel using a number mean diameter method correlated well with the single crystal growth data, 2.43 and 2.14 µm min^{-1}, respectively at $\sigma = 0.157$. This trend was also observed for the lower supersaturation, $\sigma = 0.105$, and hence provides confidence in this analysis.

Furthermore, the growth rate of ibuprofen in absolute ethanol at 750-mL process scale was reported by Rashid et al. [9] to follow a first-order dependence on supersaturation, i.e.:

$$G = k_G \sigma^n \quad \text{with } n = 1 \text{ and } k_G = 15 \tag{4}$$

where G is the linear growth rate (= dL/dt) (µm min^{-1}), L is a characteristic crystal size, here taken as the volume median size of the distribution, and k_G is the growth rate coefficient (µm/min/unit of supersaturation s).

The growth rate of ibuprofen at $\sigma = 0.157$ and 0.105 was calculated using the equation above, with results included in Tab. 1 for comparison. It is clear that the growth rate measured in the agitated vessel using the number mean diameter is of the same order as that of single crystals in stagnant solutions at a 7-mL scale and also based upon the calculated data extracted from Rashid et al. [9]. It should be noted that the data reported by Rashid et al. were collected using a laser diffraction technique and hence the growth rate data were calculated from a volumetric equivalent diameter whereas the data in this work were assessed from the area equivalent diameter. However, a comparison of the relative growth rates, particularly at the same supersaturation level, is invaluable due to the lack of measured experimental data in this field.

From the data presented in Tab. 1, it can be seen that the growth rate in the non-agitated jacketed vessel is slightly higher than that in the agitated reactors. On first examination, this result may seem somewhat counter-intuitive due to the expectation that agitation should accelerate mass transfer, diffusion, and hence the growth process. However, in this case, this effect is probably due to higher levels of secondary nucleation by contact breeding for the agitated case compared to the non-agitated case, resulting in the former crystallization environment being more likely to de-supersaturate faster. This effect is also perhaps a reflection of two growth kinetic processes proceeding simultaneously within the agitated reactor, notably the continuous formation of new crystalline particles from secondary nucleation/growth and the growth of the seed crystals.

In this case, the online measurement of the particle size through image analysis would be expected to provide an average of the constituent growth rates associated with crystal size distribution from populations of both the new nuclei (much smaller particles) and the seed crystals (larger particles). In addition, the agitation process can be expected to lead to breakage of the larger and more perfect single crystals, i.e., those having the higher growth rates, with the resultant smaller attrition fragments growing slower due to their being "less perfect" and/or more strained due to the impact of the mechanical stresses within the agitated reactor [41, 42].

This data highlight that the results of single crystal growth rate experiments can be useful in representing the growth rate of a population of crystals in an agitated crystallizer for this particular chemical system.

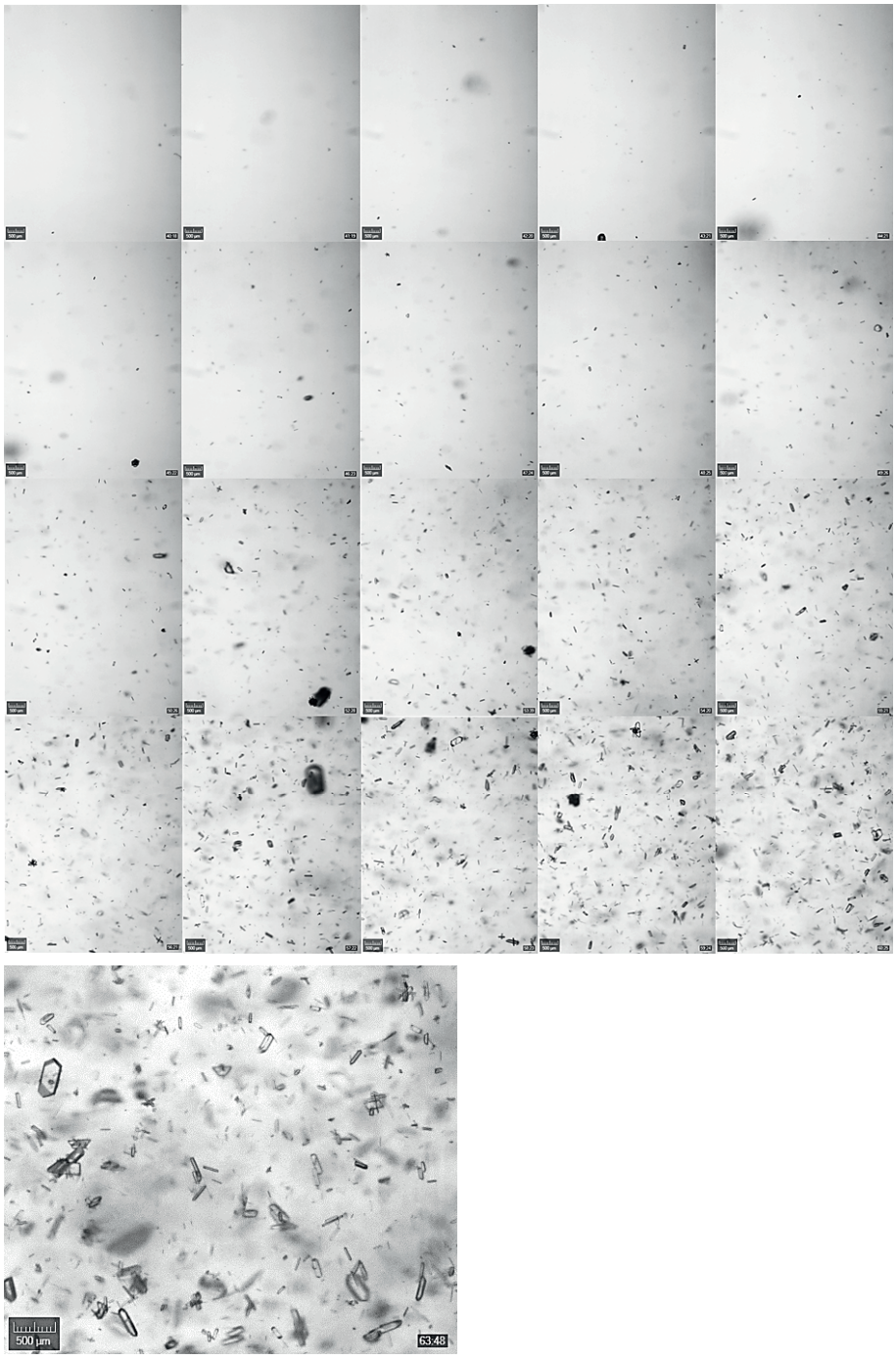

Figure 4. Real-time monitoring within the agitated vessel of the size distribution and number of crystals grown in ethanol after seeding at σ = 0.157 in an agitated reactor every 1 min (above); enlargement of an image of population of plate-like "hexagonal" morphology ibuprofen crystals (below). Scale bar: 500 µm.

4 Conclusions

This paper seeks to report preliminary crystallization science of scale data highlighting some encouraging observed correlations between the measurements of the averaged projected area equivalent diameter measured growth rates and the same when measured with less precision but at the same scale within an agitated batch reactor. Pleasingly, the data also show an acceptable degree of correlation between the experimental setups for the two supersaturations used in the measurements, which in turn were of the expected magnitude when compared to a previously published correlation which was developed at the 750-mL scale [9]. However, caution is obviously needed in generalizing the outcomes of this work, mindful that the measurements presented here are based on only a single crystallization system and for just two supersaturations.

Clearly, further work on other crystallizing systems through measurements carried out over a wider range of supersaturations and process scale sizes are needed to establish the generic significance of this kind of approach as well as to answer the question regarding the use of this science of scale methodology within routine process R&D, e.g., through its integration with population balance modeling (see the example [43]). It is hoped that the work presented here will stimulate additional interest and through this perhaps provoke further work to this overall aim.

Supporting Information

Supporting Information for this article can be found under DOI: https://doi.org/10.1002/ceat.202100025.

Acknowledgment

The authors gratefully acknowledge the financial support of this work by Pfizer and UK Northern Universities (N8) METRC initiative in molecular engineering, the UK's EPSRC for their support in nucleation research through the Critical Mass Project "Molecules, Clusters and Crystals" (EP/I014446/1 and EP/I013563/1), and the Innovate UK for funding Crystalline platform (TS/H1001638/1) used in this research.

The authors have declared no conflict of interest.

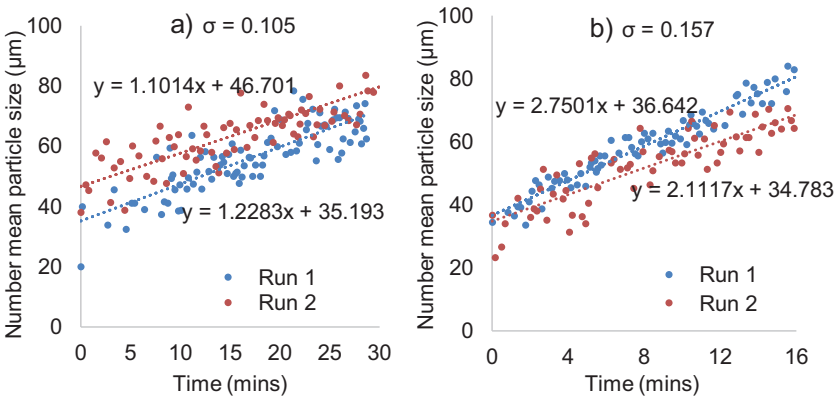

Figure 5. Crystal growth for ibuprofen in 95 % ethanol at supersaturations of 0.105 (a) and 0.157 (b) within the agitated batch crystallizer calculated from the number mean particle size distribution.

Symbols used

A	[µm^2]	calculated area of the crystals
D	[µm]	diameter for the sphere with the same area as the particle (area equivalent diameter)
$\overline{D}$	[µm]	number-weighted mean diameter
D_i	[µm]	particle size given as equivalent diameter
G	[µm min^{-1}]	crystal growth rate
k_G	[–]	growth rate coefficient
M	[g mol^{-1}]	molecular weight
x_i	[–]	number of particles in each particle size range

Greek letter

σ	[–]	relative supersaturation

References

[1] T. Nguyen, R. Hammond, K. Roberts, I. Marziano, G. Nichols, *CrystEngComm* **2014**, *16 (21)*, 4568–4586.

[2] D. R. Ochsenbein, S. Schorsch, F. Salvatori, T. Vetter, M. Morari, M. Mazzotti, *Chem. Eng. Sci.* **2015**, *133*, 30–43. DOI: https://doi.org/10.1016/j.ces.2015.02.026

[3] T. T. H. Nguyen, R. B. Hammond, K. J. Roberts, I. Marziano, G. Nichols, *CrystEngComm* **2014**, *16 (21)*, 4568–4586. DOI: https://doi.org/10.1039/C4CE00097H

[4] R. A. Judge, E. L. Forsythe, M. L. Pusey, *Cryst. Growth Des.* **2010**, *10 (7)*, 3164–3168.

[5] C. Sweegers, H. Meekes, W. Van Enckevort, I. Hiralal, A. Rijkeboer, *Cryst. Growth Des.* **2004**, *4 (1)*, 185–198.

[6] W. Omar, S. Al-Sayed, A. Sultan, J. Ulrich, *Cryst. Res. Technol.* **2008**, *43 (1)*, 22–27.

[7] S. D. Finnie, R. I. Ristic, J. N. Sherwood, A. M. Zikic, *J. Cryst. Growth* **1999**, *207 (4)*, 308–318. DOI: https://doi.org/10.1016/S0022-0248(99)00381-4

[8] Y. Tahri, E. Gagnière, E. Chabanon, T. Bounahmidi, D. Mangin, *J. Cryst. Growth* **2016**, *435*, 98–104. DOI: https://doi.org/10.1016/j.jcrysgro.2015.11.019

[9] A. Rashid, E. White, T. Howes, J. Litster, I. Marziano, *Chem. Eng. Res. Des.* **2012**, *90 (1)*, 158–161.

[10] C. Ó'Ciardhá, N. Mitchell, K. Hutton, P. Frawley, *Ind. Eng. Chem. Res.* **2012**, *51 (12)*, 4731–4740.

[11] A. Tripodi, R. Martinazzo, G. Ramis, I. Rossetti, *Chem. Eng. Technol.* **2020**, *43 (12)*, 2557–2566. DOI: https://doi.org/10.1002/ceat.202000371

[12] N. Chaisongkram, S. Maosoongnern, A. E. Flood, *Chem. Eng. Technol.* **2019**, *42 (7)*, 1519–1524. DOI: https://doi.org/10.1002/ceat.201800698

[13] X. Wang, J. Calderon De Anda, K. Roberts, R. Li, G. Thomson, G. White, *KONA* **2005**, *23*, 69–85.

[14] R. Li, G. Thomson, G. White, X. Wang, J. C. De Anda, K. Roberts, *AIChE J.* **2006**, *52 (6)*, 2297–2305.

[15] D. D. Nikolić, P. J. Frawley, *Chem. Eng. Sci.* **2016**, *145*, 317–328.

[16] V. Bhamidi, S. H. Lee, G. He, P. S. Chow, R. B. Tan, C. F. Zukoski, P. J. Kenis, *Cryst. Growth Des.* **2015**, *15 (7)*, 3299–3306.

[17] A. Ten Cate, J. Derksen, H. Kramer, G. Van Rosmalen, H. Van den Akker, *Chem. Eng. Sci.* **2001**, *56 (7)*, 2495–2509.

[18] J. Budz, P. Karpinski, Z. Nuruc, *AIChE J.* **1984**, *30 (5)*, 710–717.

[19] M. Li, G. White, D. Wilkinson, K. J. Roberts, *Chem. Eng. J.* **2005**, *108 (1–2)*, 81–90. DOI: https://doi.org/10.1016/j.cej.2005.01.005

[20] M. Torbacke, Å. C. Rasmuson, *Chem. Eng. Sci.* **2001**, *56 (7)*, 2459–2473. DOI: https://doi.org/10.1016/S0009-2509(00)00452-8

[21] X. Ni, A. Liao, *Chem. Eng. J.* **2010**, *156 (1)*, 226–233. DOI: https://doi.org/10.1016/j.cej.2009.10.045

[22] S. Khan, C. Y. Ma, T. Mahmud, R. Y. Penchev, K. J. Roberts, J. Morris, L. Özkan, G. White, B. Grieve, A. Hall, P. Buser, N. Gibson, P. Keller, P. Shuttleworth, C. J. Price, *Org. Process Res. Dev.* **2011**, *15 (3)*, 540–555. DOI: https://doi.org/10.1021/op100223a

[23] H. Cano, N. Gabas, J. Canselier, *J. Cryst. Growth* **2001**, *224 (3)*, 335–341.

[24] R. Davey, W. Fila, J. Garside, *J. Cryst. Growth* **1986**, *79 (1)*, 607–613.

[25] R. Davey, J. Mullin, *J. Cryst. Growth* **1974**, *26 (1)*, 45–51.

[26] R. Davey, J. Mullin, *J. Cryst. Growth* **1974**, *23 (2)*, 89–94.

[27] R. Davey, J. Mullin, *J. Cryst. Growth* **1975**, *29 (1)*, 45–48.

[28] S. Suharso, *J. Mat. Sains* **2009**, *10 (3)*, 101–106.

[29] A. G. Stapley, C. Himawan, W. MacNaughtan, T. J. Foster, *Cryst. Growth Des.* **2009**, *9 (12)*, 5061–5068.

[30] Y.-H. Luo, G.-G. Wu, B.-W. Sun, *J. Chem. Eng. Data* **2013**, *58 (3)*, 588–597.

[31] C. Y. Ma, X. Z. Wang, K. J. Roberts, *Adv. Powder Technol.* **2007**, *18 (6)*, 707–724.

[32] X. Wang, J. Calderon De Anda, K. Roberts, *Chem. Eng. Res. Des.* **2007**, *85 (7)*, 921–927.
[33] L. Derdour, C. Sivakumar, D. Skliar, S. Pack, C. Lai, J. Vernille, S. Kiang, *Cryst. Growth Des.* **2012**, *12 (11)*, 5188–5196.
[34] A. Markande, A. Nezzal, J. Fitzpatrick, L. Aerts, *Part. Sci. Technol.* **2009**, *27 (4)*, 373–388.
[35] A. J. Mahajan, C. J. Orella, D. Kirwan, *AIChE Symp. Ser.* **1991**, *87 (284)*, 143–153.
[36] D. L. Klug, R. L. Pigford, *Ind. Eng. Chem. Res.* **1989**, *28 (11)*, 1718–1725.
[37] www.crystallizationsystems.com/Crystalline (Accessed on December 06, 2017)
[38] T. T. H. Nguyen, I. Rosbottom, I. Marziano, R. B. Hammond, K. J. Roberts, *Cryst. Growth Des.* **2017**, *17 (6)*, 3088–3099. DOI: https://doi.org/10.1021/acs.cgd.6b01878
[39] R. E. Gordon, S. I. Amin, Crystallization of Ibuprofen, *US4476248A*, **1984**.
[40] J. Bunyan, N. Shankland, D. Sheen, *AIChE Symp. Ser.* **1991**, *87 (284)*, 44–57.
[41] J. N. Sherwood, R. I. Ristic, *Chem. Eng. Sci.* **2001**, *56 (7)*, 2267–2280. DOI: https://doi.org/10.1016/S0009-2509(00)00456-5
[42] R. I. Ristić, J. N. Sherwood, K. Wojciechowski, *J. Cryst. Growth* **1988**, *91 (1)*, 163–168. DOI: https://doi.org/10.1016/0022-0248(88)90382-X
[43] C. Ma, K. Roberts, *Ind. Eng. Chem. Res.* **2018**, *57 (48)*, 16379–16394.

